ChemPubSoc Europe

DOI: 10.1002/slct.201600023

Chemistry SELECT Communications

Electro, Physical & Theoretical Chemistry

Scaled–up sonochemical microreactor with increased efficiency and reproducibility

Bram Verhaagen,[b] Youlin Liu,[c] Andrés Galdames Pérez,[d] Elena Castro-Hernandez,[d] and David Fernandez Rivas*[a]

Bubbles created with ultrasound from artificial microscopic crevices can improve energy efficiency values for the creation of radicals; nevertheless it has been conducted so far only under special laboratory conditions. Limited reproducibility of results and poor energy efficiency are constraints for the sonochemistry and ultrasonics community to scale-up applied chemical processes. For the first time, using conventional ultrasonic bath technology, the numbering-up and scale-up of a microfluidic sonochemical reactor has been achieved. Sonochemical effects such as radical production and sonochemiluminescence were intensified by the modification of the inner walls of a novel Cavitation Intensification Bag. While 25 times bigger than the previous microreactor, a reduction of 22% in standard deviation and an increase of 45.1% in efficiency compared to bags without pits were obtained. Mechanical effects accompanying bubble collapse lead to two distinct types of erosion marks observed in the bags.

Cavitation, the formation and collapse of bubbles in liquids, has been used as a green energy-focusing tool to produce chemical effects (notably production of free radicals), enhanced luminescence, mechanical activation of heterogeneous systems, physicochemical modifications of inert materials as well as water remediation, water splitting, and bioenergy applications.[1] These effects can all be harnessed in applied domains, from cleaning to water treatment and nanochemistry. However, a main barrier for sonochemical and ultrasonic reactors to be utilized for industrial purposes and other uses is the lack of reproducibility, along with a low energy efficiency.[2]

Employing the same ultrasonic equipment, glassware, chemicals and experimentalist person, is no guarantee that the standard deviations of an expected result will be small. This lack of reproducibility is because creating bubbles with ultrasound closely resembles a stochastic process, depending on physical-chemical factors difficult to control at once.[3] The first is the nucleation sites from which bubbles are created. Once bubbles are nucleated, liquid-gas concentration, frequency and amplitude of ultrasound signal, etc. have a significant influence on the overall cavitation process. These parameters influence the "unitary" reactor that a bubble itself represents, and determine the generation of plasma conditions, sonoluminescence, shockwaves, jetting, and radical production, upon collapse.[4] Despite all these useful phenomena available at ambient pressure and room temperature, industrial applications have been hindered due to a meager $\sim 10^{-6}$-10^{-5} (kg/kJ) energy efficiency of cavitation reactors.[5]

The present work is motivated by the challenge in scaling-up a microfluidic sonochemical reactor while increasing its results reproducibility.[6] The energy efficiency of that system was calculated as the product of radical formation rate and the energy required for the formation of $OH^{\cdot}$ radicals divided by the electric power absorbed by the transducer. With only three small artificial bubble nucleation sites (crevices, pits), 10 times higher energy efficiencies were reached.[7] Nevertheless, the total radical production was limited to a volume of ~250 μL, far from interesting for large scale uses. Other ways to influence cavitation have also been reviewed in literature.[8]

We present a novel sonochemical reactor concept, the Cavitation Intensification Bag (CIB),[9] which has pits indented onto the inner surface of a plastic bag. When liquid is added and the bag is placed inside an ultrasonic bath, the 900 ± 30 pits allow for intensification of the amount of cavitation in a well-defined manner. In Figure 1a clusters of bubbles can be seen to originate from the pits upon exposure to ultrasound. Some of the clusters are found to interact with the CIB walls and other clusters, forming distinct patterns.

Sonochemiluminescence is widely used to demonstrate local radical creation.[10] The $OH\bullet$ radicals produced by cavitation react with luminol in solution, giving blue light. In Figure 1b, intense blue areas can be observed connected to the regular indentation pattern on the CIB surface. The light intensity corresponds with higher radical production zones inside the CIB.

[a] *Dr. D. Fernandez Rivas*
Mesoscale Chemical Systems
University of Twente
P.O.Box 217, 7500AE Enschede, The Netherlands
ORCID 0000–0003-4329-3248
E-mail: d.fernandezrivas@utwente.nl
[b] *Dr. B. Verhaagen*
BuBclean
Institutenweg 25, 7521PH Enschede, The Netherlands
[c] *Y. Liu*
School of Chemistry and Materials Science
University of Science and Technology of China
Jinzhai Road 96, Hefei 230026, Anhui Province, P. R. China
[d] *A. G. Pérez, Dr. E. Castro-Hernandez*
Area de Mecanica de Fluidos
Universidad de Sevilla
Avenida de los Descubrimientos s/n 41092, Sevilla, Spain

Supporting information for this article is available on the WWW under http://dx.doi.org/10.1002/slct.201600023

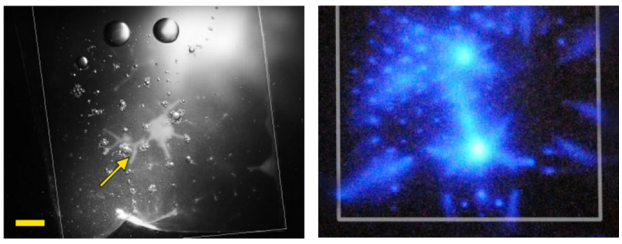

Figure 1. (left) Photograph of bubble clouds inside a CIB; (right) sonochemiluminescence (blue) inside a CIB. The arrow indicates the bubble clouds originating from the pits; the scale bar represents 5 mm.

Terephthalic acid dosimetry was used for quantification of the radicals produced inside the CIB and inside bags without pits (see Supporting Information).[5] After 5 minutes inside the CIB, the amount of radicals produced had increased with 33% and the scattering of the data was reduced with 22% compared to bags without pits (Figure 2); an evidence of improved

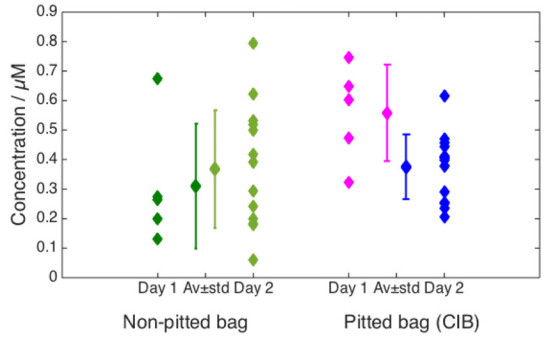

Figure 2. Radical production after 5 min sonication measured on two different days (different colors) in bags with/without pits. The average concentration value is higher for the case with pits, and the dispersion in experimental results is drastically reduced compared to the case of no pits.

reproducibility of sonochemistry. The production of radicals increases with time, and this increase is even faster for bags with pits than without pits. After 15 minutes, the amount of radicals produced is increased by up to 133% compared to bags without pits. The reaction rate decreases with time (Figure 3).

For bags without pits, the amount of radicals produced is similar for both bag materials poly-propylene (PP) and polyethylene (PE). When comparing bags with pits, PP bags produce 3 times more radicals than PE bag. We expect this to be due to the different production methods of PP and PE bags, resulting in different pit geometries. Reuse of the bag (after cleaning with milliQ water and drying with pressurized nitrogen) resulted in 15% higher spreading of the amount of radicals produced. In some cases the production of radicals surprisingly increased compared to new bags; possibly due to the fact that, despite cleaning thoroughly the interior of all bags, some residues might still exist that alters the measured value; for this reason, new bags should be used for highest reproducibility.

Comparing results of sonochemical and ultrasonic studies in literature is a difficult challenge because of the variety in equipment, settings and parameters. We chose power density (W/L), frequency and pressure values of ultrasound. Two ultrasonic baths operating at 35 kHz (24.2 W/L) and at 45 kHz (33.3 W/L) were used, corresponding to a 37.7% difference in power density. We found that up to 117% more radicals are produced at higher frequency and power, in accordance with literature.[11] In order to compare the radical production in the CIB with other systems, the pressure amplitude at the location of the CIB inside the ultrasonic baths was measured. Using a hydrophone calibrated at 39 KHz, the pressure was found to be around 364 kPa in the large ultrasonic bath, and up to 427 KPa in the small ultrasonic bath, with an uncertainty in the pressure amplitude of 24%. The 50 μm thick bags allow for 79.4-86.0% of the ultrasound to be transmitted to the contained liquid.

Compared to the radical production rate of 10^{-2} μM s^{-1} in the microfluidic sonochemical reactor of previous studies, the CIB bags produce radicals at a rate one order of magnitude smaller, despite having 300 times more pits. Following a methodology described previously,[6] we calculated the energy efficiency for the bags with and without pits, taking into account the radical production rate within the 5 mL of liquid inside the bags, after 5 minutes of sonication. We found that the system as a whole has an efficiency on the order of 10^{-8} to 10^{-7} (Table 1), not taking into account radicals formed outside the CIB.

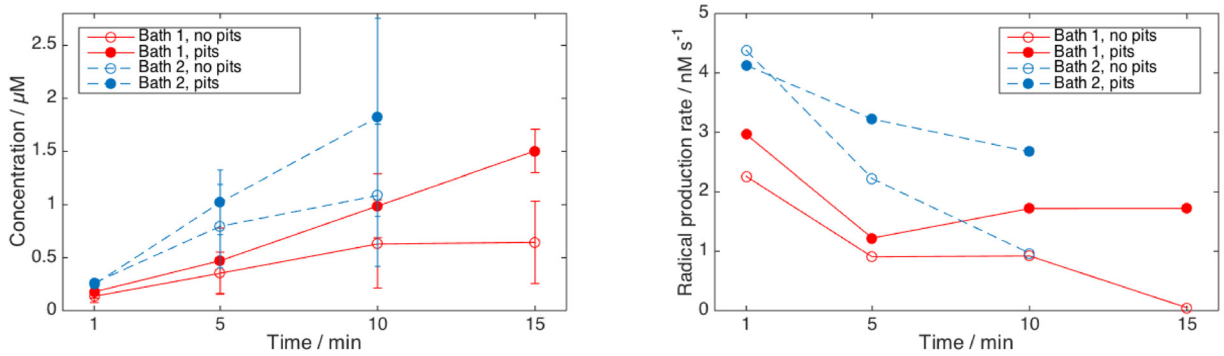

Figure 3. (a) Radical production in bags with/without pits, as a function of time and for a large and a small ultrasonic bath (Bath 1 and 2, respectively). (b) Rate of radical production.

Table 1. Energy efficiencies[a] calculated for the two baths and two types of bags, after 5 minutes of sonication.

	Bath 1		Bath 2	
	Non-pitted bag	CIB	Non-pitted bag	CIB
Efficiency (10^{-8})	1.4 ± 0.8	1.9 ± 1.2	9.1 ± 6.4	13.2 ± 4.9
Efficiency (10^{-5}), corrected for bath volume	1.8 ± 1.0	2.5 ± 1.6	3.3 ± 2.3	4.7 ± 1.7

[a] Efficiencies E were calculated using the following formula: $E = \frac{\Delta H \cdot dN/dt}{P_{US}}$

where ΔH is the energy required for the formation of $OH^{\bullet}$ radicals (5.1 eV per molecule), dN/dT radical formation rate in moles per second, and P_{US} the electrical power consumed by the ultrasonic bath.

The CIB contributes to an increase of the efficiency up to 45.1% compared to bags without pits. However, the absolute efficiency is low even compared to standard ultrasound reactors, which is due to the fact that the ultrasonic baths dissipate the acoustic energy throughout the bath volume and not just the bag volume. When we correct the ultrasonic power by reducing it by the ratio of bag volume to bath volume, we find efficiencies up to 4.7×10^{-5}. Here we assumed that the ultrasonic energy is distributed equally throughout the bath volume, which is not the case in practice – therefore the estimated efficiency may even be underestimated. This result shows that we not only scaled up the microreactor 25 times, but also achieved a potential five-fold increase of its efficiency. The presence of pits inside the CIB contributes to cavitation in places that otherwise would have had no radical production, as shown in Figure 1 and Supporting Information movie 1. This is a verification that pits on the walls of sonochemical reactors serve as process intensification tool.

After exposure to ultrasound for 15 minutes we observed inside some CIBs characteristic sub-millimeter white spots in random locations (Supporting Information Figure S1). We denote type A those found on places in the proximity of the pits, and the erosion type B as those shapes distant from the pits, which resemble erosion observed in previous studies with silicon substrates. We have no evidence that this type of erosion in the bag walls could serve as new nucleation sites. Images taken with Scanning Electron Microscopy show two distinct types of surface topography (Figure 4). Erosion type A consisted of distinct patterns of small pits (diameter on the order of 1 μm) in the plastic surface. The patterns originated from one to four adjoining pits, and may be a material fatigue effect due to the frequent collapse of bubbles.[7] Erosion type B consisted of larger areas of about 100 μm in diameter exhibiting plastic deformation, with protruding or recessed features on the surface. We hypothesize that these features appear when the walls of the CIB touch each other. A bubble (or cluster of bubbles) may locally heat up the plastic, thereby melting the two walls together. Sometimes a small force was required to open the CIB after use, indicating that the walls indeed bonded. This interesting observation indicates the existance of 'hot zones' generated by bubbles active for several minutes on specific zones. In these 'hot zones', the temperature is higher than the average bath temperature (below 299 K), but much lower than the temperatures at the bubble interior during collapse (more than 5000 K). Commercial grades of polyethylene melting point are reported around 400 K; further investigations will be needed to verify if at those particular spots the local temperature of the liquid might have reached the melting point. Other studies have looked into oxidation and other effects on polymers (PE) exposed to ultrasound and also reported microscopic effects. Penetration of oxidation was found within 1 μm of the surface depth, yet the amount of radicals produced could not fully explain the enhanced oxidation and modifications of the surface. It was speculated on how bubble collapses can produce local heating and surface deformations, although polymer chain breakage could not be detected.[12] Future studies in this direction can be helpful in the activation of inert polymers.

We conclude that the reproducibility of sonochemical processes, particularly radical production, can be improved with artificial nucleation sites. Using conventional ultrasonic equipment and procedures, a sonochemical microreactor was scaled-up allowing for processing 25 times more volume with a potential five-fold increase in efficiency. While the current sonicated volumes are still low for industrial processes, it provides insight on how to scale-up microreactors, and is a necessary step for future sonochemical efficiency and reproducibility improvements.

Acknowledgements

We thank M. Smithers for assistance with SEM analysis, Prof. J. Huskens for the spectroscopy measurements access, Dr. G. Lajoinie for contributing to the pressure measurements, and Prof. P. Cintas for helpful discussions. We gratefully acknowledge the China scholarship Council (CSC) for providing scholarship for the internship of Y. Liu.

Keywords: sonochemistry · ultrasound · radicals · intensification · bubbles

[1] a) P. Cintas, *Ultrason. Sonochem.* **2016**, *28*, 257–258; b) G. Cravotto, P. Cintas, *Angew. Chem. Int. Ed.* **2007**, *46*, 5476–5478; c) P. A. May, J. S. Moore, *Chem. Soc. Rev.* **2013**, *42*, 7497–7506; d) P. Cintas, G. Cravotto, A. Barge, K. Martina, in *Polymer Mechanochemistry* (Ed.: R. Boulatov), *Topics in Current Chemistry*, Vol. 369, Springer, Berlin, **2015**, pp. 239–284. e) H. Wang, *Energy Environ. Sci.*, **2013**, 6 (3), pp. 799–804; f) J.A. Choi, *Energy Environ. Sci.* **2011**, 4 (9), pp. 3513–3520.

[2] a) A. A. Ndiaye, R. Pflieger, B. Siboulet, S. I. Nikitenko, *Angew. Chem. Int. Ed.* **2013**, *52*, 2478–2481; b) E. V. Skorb, D. V. Andreeva, H. Möhwald, *Angew. Chem. Int. Ed.* **2012**, *51*, 5138–5142; c) R. Xiao, D. Diaz-Rivera, Z. He, L. K. Weavers, *Ultrason. Sonochem.* **2013**, *20*, 990–996; d) P. R. Gogate, V. S. Sutkar, A. B. Pandit, *Chem. Eng. J.* **2011**, *166*, 1066–1082; e) J. H. Bang, K. S. Suslick, *Adv. Mater.* **2010**, *22*, 1039–1059; f) C. Leonelli, T. J. Mason, *Chem. Eng. Process.* **2010**, *49*, 885–900.

[3] T. G. Leighton, *Ultrasonics Sonochemistry* **1995**, *2*, S123–S136.

[4] a) D. Lohse, *Nature* **2005**, *434*, 33–34; b) D. J. Flannigan, K. S. Suslick, *Nature* **2005**, *434*, 52–55.

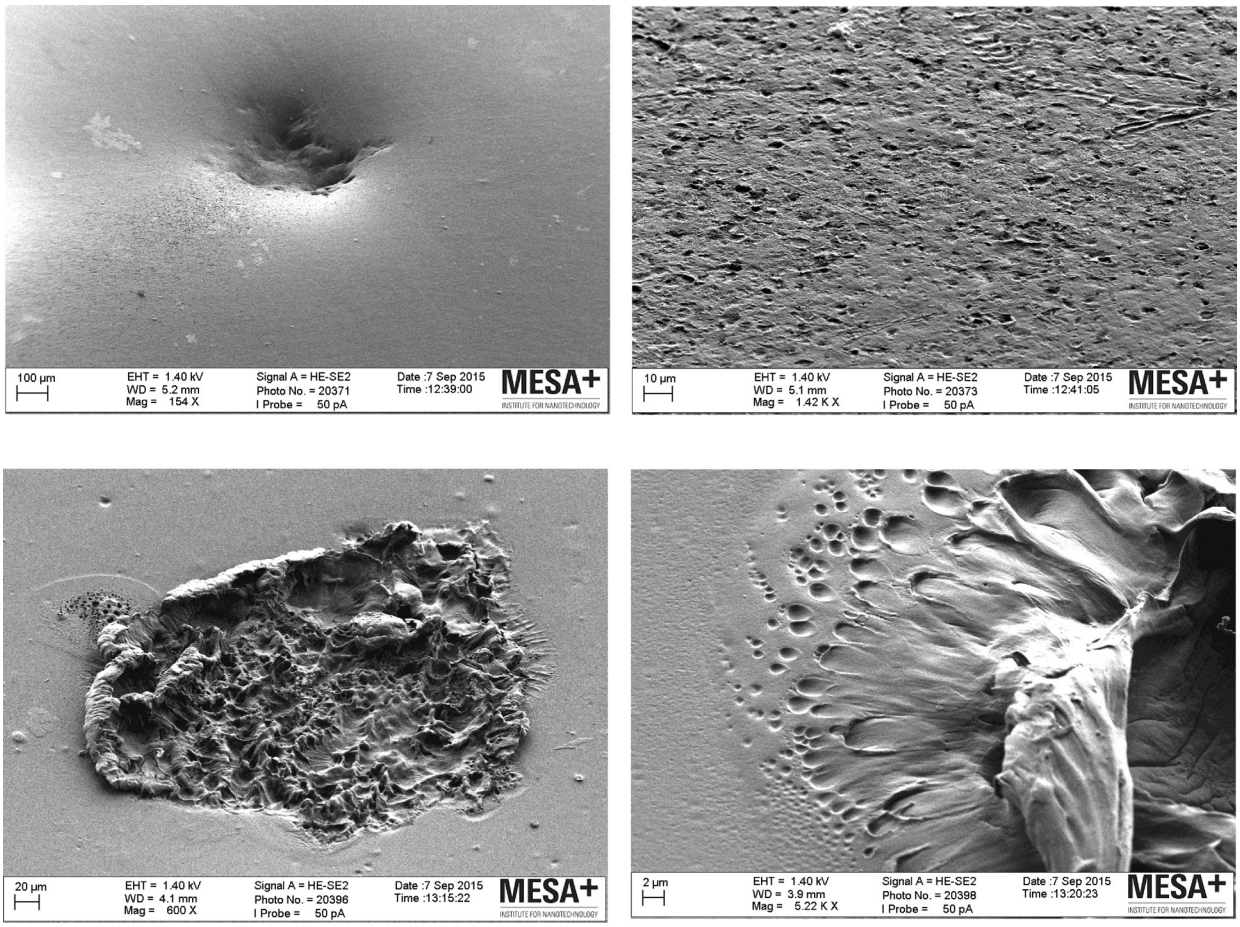

Figure 4. SEM images of the two types of erosion: type A (top two panels) consisting of small erosion pits, and type B (bottom two panels) featuring large deformations.

[5] a) Y. T. Didenko, K. S. Suslick, *Nature* **2002**, *418*, 394–397; b) A. Stankiewicz, *Chem. Eng. Res. Des.* **2006**, *84*, 511–521.
[6] D. Fernandez Rivas, A. Prosperetti, A. G. Zijlstra, D. Lohse, H. J. G. E. Gardeniers, *Angew. Chem. Int. Ed.* **2010**, *49*, 9699–9701.
[7] a) D. Fernandez Rivas, L. Stricker, A. G. Zijlstra, H. J. G. E. Gardeniers, D. Lohse, A. Prosperetti, *Ultrason. Sonochem.* **2013**, *20*, 510–524; b) D. Fernandez Rivas, J. Betjes, B. Verhaagen, W. Bouwhuis, T. C. Bor, D. Lohse, J. G. E. Gardeniers, *J. Appl. Phys.* **2013**, *113*, 064902.
[8] a) N. Bremond, M. Arora, C.-D. Ohl, D. Lohse, *Phys. Rev. Lett.* **2006**, *96*, 224501; b) V. Belova, D. A. Gorin, D. G. Shchukin, H. Möhwald, *Angew. Chem. Int. Ed.* **2010**, *49*, 7129–7133; c) D. G. Shchukin, E. Skorb, V. Belova, H. Möhwald, *Adv. Mater.* **2011**, *23*, 1922–1934.
[9] D. Fernandez Rivas, B. Verhaagen, A. Galdamez Perez, E. Castro-Hernandez, R. van Zwieten, K. Schroen, *J. Phys.: Conf. Ser.* **2015**, *656*, 012112.
[10] a) M. Zhou, N. S. M. Yusof, M. Ashokkumar, *RSC Adv.* **2013**, *3*, 9319–9324; b) D. Fernandez Rivas, M. Ashokkumar, T. Leong, K. Yasui, T. Tuziuti, S. Kentish, D. Lohse, H. J. G. E. Gardeniers, *Ultrason. Sonochem.* **2012**, *19*, 1252–1259; c) R. G. Macedo, B. Verhaagen, D. Fernandez Rivas, H. J. G. E. Gardeniers, L. W. M. Van der Sluis, P. R. Wesselink, M. Versluis, *Ultrason. Sonochem.* **2014**, *21*, 324–355.
[11] a) T. J. Mason, A. J. Cobley, J. E. Graves, D. Morgan, *Ultrason. Sonochem.* **2011**, *18*, 226–230; b) G. Cravotto, E. C. Gaudino, P. Cintas, *Chem. Soc. Rev.* **2013**, *42*, 7521–7534; c) V. S. Sutkar, P. R. Gogate, *Chem. Eng. J.* **2009**, *155*, 26–36; d) I. Hua, M. R. Hoffmann, *Environ. Sci. Technol.* **1997**, *31*, 2237–2243.
[12] a) G. J. Price, F. Keen, A. A. Clifton, *Macromolecules* **1996**, *29*, 5664–5670; b) Y. Zhao, C. Bao, R. Feng, T. J. Mason, *J. Appl. Polym. Sci.* **1998**, *68*, 1411–1416.

Submitted: January 13, 2016
Accepted: January 22, 2016